Characterization of the Physicochemical Parameters of Dense Core Atrial Gland and Lucent Red Hemiduct Vesicles in Aplysia c alifornica

ARTICLE *in* ANALYTICAL CHEMISTRY · MAY 2004

Impact Factor: 5.64 · DOI: 10.1021/ac035346h · Source: PubMed

6 AUTHORS, INCLUDING:

Luisa Ciobanu
Atomic Energy and Alternative Energies Com…
53 PUBLICATIONS **634** CITATIONS
SEE PROFILE

Stanislav S Rubakhin
University of Illinois, Urbana-Champaign
112 PUBLICATIONS **2,750** CITATIONS
SEE PROFILE

Jonathan Sweedler
University of Illinois, Urbana-Champaign
511 PUBLICATIONS **15,112** CITATIONS
SEE PROFILE

Anal. Chem. **2004,** *76,* 2331−2335

Characterization of the Physicochemical Parameters of Dense Core Atrial Gland and Lucent Red Hemiduct Vesicles in *Aplysia californica*

Luisa Ciobanu,[†,‡] Stanislav S. Rubakhin,[‡,§] Jeffrey N. Stuart,[‡,§] Robert R. Fuller,[‡,§,||] Andrew G. Webb,[*,†,‡] and Jonathan V. Sweedler[*,‡,§]

Department of Electrical and Computer Engineering, University of Illinois at Urbana−Champaign, 1406 West Green Street, Urbana, Illinois 61801, Beckman Institute, University of Illinois at Urbana−Champaign, 405 North Mathews Avenue, Urbana, Illinois 61801, and Department of Chemistry, University of Illinois at Urbana−Champaign, 600 South Mathews Avenue, Urbana, Illinois 61801

Characterizing femtoliter-volume cellular organelles requires innovative analytical techniques such as mass spectrometry, separations, and NMR. The capabilities of all three are demonstrated for characterizing the physicochemical properties of the electron-dense core atrial gland vesicles from *Aplysia californica* and comparing them with the same properties of the electron lucent red hemiduct vesicles. Single-vesicle mass spectrometric measurements show that the atrial gland vesicles contain an abundance of peptides while the red hemiduct vesicles contain no detectable peptide signals. Capillary electrophoresis with wavelength-resolved native fluorescence detection is used to characterize larger vesicle samples for tyrosine- and tryptophan-containing peptides. Using NMR spectroscopy, we show that the physiologically active peptides located in the core of the atrial gland vesicles are NMR inactive when the vesicles are intact. Resonances from these peptides appear after vesicle lysis by heating, suggesting that initially they are packed in a crystalline or semicrystalline core so that the NMR resonances are not detectable. In contrast, the red hemiduct vesicles appear to have their contents stored in a completely mobile form due to the fact that no new NMR resonances are detected after heating.

Secretory vesicles are specialized intracellular organelles functionally involved in mechanisms of intercellular and interorganism chemical communication. Higher eukaryotic organisms generate secretory vesicles that play important roles in organism functioning including learning and memory. Two major types of vesicles are distinguished by their morphology—dense core and lucent vesicles. Dense core vesicles (DCVs) exhibit an electron-opaque central region and generally contain peptides or proteins. Lucent vesicles (LVs) are more transparent to electron microscopy and are usually packed with small signaling molecules such as serotonin, dopamine, and acetylcholine. Although the biochemistry and morphology of secretory vesicles have been well studied, little is known about the physicochemical parameters of the intravesicular contents. This lack of knowledge restricts temporal and spatial modeling of the packaging of signaling molecules as well as of the dynamics of their release and consequently the understanding of physiolological and pathophysiological processes that involve DCVs.

Nuclear magnetic resonance (NMR) spectroscopy is a versatile analytical method that can provide information about the physicochemical properties of the intravesicular content of intact DCVs. NMR has been used previously to study the physical state of histamine in mast cells and in mast cell granules[1] and to determine the chemical composition of the aqueous phase of bovine chromaffin granules.[2−4] Chromaffin granules are adrenal gland organelles that contain the catecholamines epinephrine and norepinephrine. A comparison of the analyte concentrations from lysed vesicles with NMR results showed that high concentrations of the catecholamines and adenosine triphosphate (ATP) are dissolved in the aqueous phase of a partially ionic environment. No significant ordered phases were detected inside these vesicles. The lack of strong interaction between ATP, catecholamines, and Ca^{2+} revealed by several NMR studies[5,6] suggested the existence of distinct compartments within the chromaffin granules. This hypothesis has been confirmed by Ornberg et al., who found small, membrane-bound structures within these granules.[7] Such intergranular vesicles can also be found in other systems besides chromaffin cells. As one example, pancreatic β-cell secretory granules have a dense core of concentrated, presumably solid, insulin.[8] However, the β-cell secretory granule cores have an irregular-

† Department of Electrical and Computer Engineering.
‡ Beckman Institute.
§ Department of Chemistry.
|| Present address: Mercer University, Macon, GA 31207.

(1) Rabenstein, D. L.; Ludowyke, R.; Lagunoff, D. *Biochemistry* **1987**, *26*, 6923−6926.
(2) Sen, R.; Sharp, R. R.; Domino, L. E.; Domino, E. F. *Biochim. Biophys. Acta* **1979**, *587*, 75−88.
(3) Daniels, A. J.; Williams, R. J. P.; Wright, P. E. *Nature* **1976**, *261*, 321−323.
(4) Sharp, R. R.; Richards, R. E. *Biochim. Biophys. Acta* **1977**, *538*, 155−163.
(5) Pollard, H. B.; Shindo, H.; Creutz, C. E.; Pazoles, C. J.; Cohen, J. S. *J. Biol. Chem.* **1979**, *254*, 1170−1177.
(6) Sen, R.; Sharp, R. R. *J. Biochem.* **1981**, *195*, 329−332.
(7) Ornberg, R. L.; Duong, L. T.; Pollard, H. B. *Cell Tissue Res.* **1986**, *245*, 547−553.
(8) Bendayan, M.; Roth, J.; Perrelet, A.; Orci, L. *J. Histochem. Cytochem.* **1980**, *28*, 149−160.

10.1021/ac035346h CCC: $27.50
Published on Web 03/04/2004

shaped presumed crystalline core, different from the more typical DCV smooth spherical core.

Due to their micrometer size,[9] well-characterized chemistry, and morphology,[10−13] as well as abundance and homogeneity inside the source organ, the atrial gland DCVs of the marine slug *Aplysia californica* represent a unique model for the study of the physical state of the vesicular dense core. *A. californica* is a major neurobiological model for the investigation of the role of peptides as neurohormones and regulators of behavior.[14−16] Immunogold histochemical approaches and electron microscopy have demonstrated that signaling peptides are located in the electron-opaque dense core, while the processing enzymes are located in a halo near the lipid bilayer.[9] However, little is known about the physical state of the peptides in the dense cores of these vesicles as well as in a plethora of other DCVs. *A. californica* also provides an attractive model for the study of LVs in the form of red hemiduct vesicles. These vesicles are similar in size to atrial gland DCVs. However, they do not possess dense cores or significant amounts of peptides and therefore represent an excellent model for comparative investigation of DCVs and LVs.

In this study, we characterize the internal state of the contents of DCVs and LVs by performing high-resolution proton NMR spectroscopy. We apply two approaches to characterize individual vesicles—transmission electron microscopy (TEM) and matrix-assisted laser desorption/ionization mass spectrometry (MALDI-MS). In addition, capillary electrophoresis (CE) with wavelength-resolved laser-induced native fluorescence is used with larger vesicle samples. These approaches add structural and chemical information to the physicochemical NMR data. The results of our investigation indicate that the atrial gland signaling peptides are packed in a semisolid or solid dense core and also demonstrate the large differences in contents and structure between the red hemiduct and dense core atrial gland vesicles.

EXPERIMENTAL SECTION

Materials. Unless otherwise stated, all reagents and standards were obtained from Sigma Chemical Co. (St. Louis, MO) without further purification and are of analytical grade or higher. Artificial seawater (ASW) consisted of the following components: NaCl (460 mM), KCl (10 mM), $CaCl_2$ (10 mM), $MgCl_2$ (22 mM), $MgSO_4 \cdot 7\ H_2O$ (26 mM), and HEPES (10 mM), pH 7.8. A pH 8.8 borate buffer for the CE assays was prepared by dissolving 3.0 g of boric acid (H_3BO_3) and 9.2 g of sodium borate ($Na_2B_4O_7 \cdot 10H_2O$) in 1 L of ultrapure water (Milli-Q filtration system; Millipore, Bedford MA).

Vesicle Preparation. Red hemiduct (RH) lucent vesicles and atrial gland (AG) dense core vesicles were dissected from the hermaphroditic ducts of adult 400−600 g *A. californica*. These structures were placed for 10 min in separate dishes containing ASW−antibiotic solution. To reduce the complexity of the extravesicular matrix, which may interfere with NMR analysis of vesicle contents, AG and RH vesicles were washed twice for ∼10 min in buffer containing 0.5 M NaCl and 1 mM thimerosal dissolved in D_2O. Thimerosal was used as an antibiotic and as an internal standard for NMR measurements. AG and RH vesicles were transferred to dry individual vials where they were cut into small pieces using surgical scissors. A volume of 500 μL of buffer was added to each vial. After centrifugation at 600 rpm for 8 min, the supernatant was removed and transferred to new vials and centrifuged for a second time at 2000 rpm for 5 min. At the end of sample preparation, the pellet contained mainly AG or RH vesicles. The supernatant was carefully replaced with fresh buffer, and the vesicles were transferred to 190-μL NMR microcell inserts (Wilmad-Labglass, Buena, NJ) filled with buffer in advance. The entire vesicle isolation process was carried out at room temperature.

Transmission Electron Microscopy Procedure. The AG and RH tissues were placed immediately after dissection into 4% glutaraldehyde in ASW or in modified Karnovsky's fixative at 4 °C for at least 8 h. After fixation and storage, the tissue was rinsed with cacodylate buffer and stained with 2% OsO_4 solution for up to 30 min in a rotator. The tissue was then removed and dehydrated with solutions of increasing concentrations of ethanol up to 100% ethanol. The infiltration was performed with Araldite 502 epoxy resin. The epoxy and sample were subsequently transferred to a BEEM capsule and epoxy polymerized at 50 °C for 8−12 h. Following thin-sectioning with a diamond knife, 70−90-nm-thick tissue sections were placed on a 300-mesh copper grid and end-block stained with uranyl acetate followed by lead citrate. TEM was performed on a Hitachi-600 electron microscope (Center for Electron Microscopy, UIUC) operating at 75−80 kV.

Mass Spectrometry of Individual Secretory Vesicles. Detailed protocols of single-vesicle isolation and profiling are described elsewhere.[17] Briefly, vesicles were isolated from tissue, attached to a glass surface, and washed with 1 M NaCl solution. Individual vesicles were transferred to a clean glass spot, and the extracellular buffer was quickly removed. An inverted microscope (100× oil objective with a Zeiss Axiovert 100 × 1000 magnification) adjusted for phase contrast and a glass micropipet controlled by a micromanipulator (Narishege, Tokyo, Japan) were used for the deposition of ∼10 pL of MALDI matrix (α-cyano-4-hydroxycinnamic acid saturated in a 3:2 mixture of acetonitrile/0.1% (v/v) aqueous trifluoroacetic acid) onto the dried vesicle. All MALDI mass spectra are acquired using a Voyager DE-STR time-of-flight mass spectrometer (PE Biosystems, Foster City, CA). The desorption/ionization laser (337 nm) was focused to a ∼25-μm-diameter spot size by placing a pinhole aperture in front of the instrument's standard focusing optical setup.

Capillary Electrophoresis with Wavelength-Resolved Laser-Induced Native Fluorescence Detection. A laboratory-assembled CE system with 257-nm excitation and a charge-coupled device (CCD)/spectrograph was used for these studies.[18−21]

(9) Kreiner, T.; Sossin, W.; Scheller, R. H. *J. Cell Biol.* **1986**, *102*, 769−782.
(10) Rothman, B.; Hawke, D.; Brown, R.; Lee, T.; Deghan, A.; Shively, J.; Mayery, E. *J. Biol. Chem.* **1986**, *261*, 1616−1623.
(11) Nagle, G. T.; Painter, S. D.; Blankenship, J. E.; Kurosky, A. *J. Biol. Chem.* **1988**, *263*, 9223−9237.
(12) Lillard, S. J.; Chiu, D. T.; Scheller, R. H.; Zare, R. N.; Rodriguez-Cruz, S. E.; Williams, E. R.; Orwar, O.; Sandsberg, M.; Lundqvist, J. A. *Anal. Chem.* **1998**, *70*, 3517−3524.
(13) Chiu, D. T.; Lillard, S. J.; Scheller, R. H.; Zare, R. N.; Rodriguez-Cruz, S. E.; Williams, E. R.; Orwar, O.; Sandsberg, M.; Lundqvist, J. A. *Science* **1998**, *279*, 1190−1193.
(14) Kandel, E. R.; Schwartz, J. H. *Science* **1982**, *218*, 433−443.
(15) Fraizer, W. T.; Kandel, E. R.; Kupfermann, I.; Waziri, R.; Coggeshall, R. E. *J. Neurophysiol.* **1980**, *30*, 1288−1351.
(16) Jung, L. J.; Scheller, R. H. *Science* **1991**, *251*, 1330−1335.
(17) Rubakhin, S. S.; Garden, R. W.; Fuller, R. R.; Sweedler, J. V. *Nat. Biotechnol.* **2000**, *18* (2), 172−175.
(18) Fuller, R. R.; Moroz, L. L.; Gillette, R.; Sweedler, J. V. *Neuron* **1998**, *20*, 173−181.

Briefly, a fused-silica capillary (Polymicro Technologies, Phoenix, AZ), 80-cm length, 50-μm inner diameter, 140-μm outer diameter, was employed as a separation column. The detection end of the capillary was directed into a sheath flow assembly, where the natively fluorescent analytes eluted in the core stream and were excited by a frequency-doubled, liquid-cooled argon ion laser (Innova 300 FrED; Coherent, Palo Alto, CA) operating at 257 nm. The sheath flow rate was 0.75 mm/s, and the laser power was adjusted to 0.85 mW at the sheath flow cell. The collection optics were orthogonal to the excitation beam, focusing the fluorescence emission onto a $f/2.2$ CP 140 imaging spectrograph (Instruments SA, Edison, NJ) and then onto a 1,024 $\times$ 256 detector array, liquid nitrogen-cooled scientific CCD (EEV 15-11, Essex, U.K.). The sample injection was performed electrokinetically at 2.1 kV for 10.0 s from a 360-nL stainless steel nanovial, and a ~3-nL sample was injected into the capillary. The separation voltage was maintained at 21 kV. Fluorescence emission data from 260 to 710 nm were processed and analyzed using MATLAB (Mathworks, Natick, MA). The identification of compounds was based on a comparison of both migration time and fluorescence emission spectra with commercially available standards including Trp and Tyr HCl (Sigma Chemical Co.) The wavelength-resolved laser-induced native fluorescence detection system was optimized to detect Trp and Trp-containing peptides.

NMR Spectroscopy. All NMR experiments were conducted on a 600-MHz (14.1 T) Varian Unity Inova (Varian Inc., Palo Alto, CA). NMR spectra were obtained using a 90° flip angle and a delay of 2 s. Typically 200 transients were collected. Chemical shifts were referenced to the residual HOD peak at 4.78 ppm. All NMR spectra were processed with NUTS (2D-version 19990629; Acorn NMR Inc.; Fremont, CA).

RESULTS

The major goal was to characterize two subpopulations of the cellular organelles within the atrial gland, the dense core vesicles and the red hemiduct vesicles. We have chosen tissues high in these organelles, allowing straightforward isolation. We used a combination of mass spectrometry and capillary electrophoresis to characterize their chemical content and EM to characterize their structure. Last, NMR provides unique information on the packaging of the contents of these organelles.

Electron Microscopic Characterization of DCVs and LVs. We applied transmission electron microscopy and MALDI-MS to verify and compare the morphology and the biochemistry of DCVs and LVs, as well as to confirm the nondestructive nature of the vesicle isolation procedure. Microphotographs of isolated DCVs and LVs are shown in Figure 1A, B and D, E, respectively. The electron micrographs of the DCV depict an electron dense core surrounded by a ruffled, less-electron-dense membrane (Figure 1B). No internal structure is apparent in the matrix of these vesicles. The LVs are morphologically easily distinguished from the DCVs. They appear to contain two membranes rather than a single membrane, with the inner membrane forming cristalike structures inside the vesicle (Figure 1E).

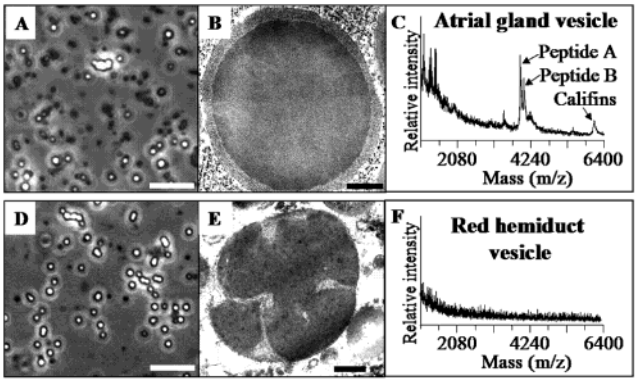

Figure 1. Morphological and biochemical examination of the atrial gland DCVs and the red hemiduct LVs. (A) Light micrograph of a purified fraction of DCVs. (B) Transmission electron micrograph of a single DCV demonstrating a dense core occupying most of the vesicle inner space. (C) Mass spectrum of an individual DCV, showing the presence of many peptides. (D) Light micrograph of a purified fraction of red hemiduct LVs. (E) Transmission electron micrograph of a single LV showing the presence of crystae and the lack of a dense core. (F) Mass spectra of an individual LV. No peptides were detected. Scale bars: 0.5 μm for (B) and (E); 10 μm for (A) and (D). Brightness and contrast of the images in (B) and (E) are individually adjusted for better visualization of the vesicle morphology. The MALDI-MS protocols were optimized for maximal sensitivity for peptide detection.

Mass Spectrometry. Using unique single-vesicle sampling protocols, the peptidergic nature of DCVs was confirmed using MS on single 0.3−3-fL vesicles. Several well-characterized peptides are detected including califins, peptides A and B (Figure 1C). No peaks are visible in the mass spectrum of a single red hemiduct vesicle (Figure 1F), suggesting that the amount of peptides inside these vesicles is below the attomole detection limits of MS.

Capillary Electrophoresis Analysis of AG Vesicles. To further characterize the content of the AG vesicles, and also to confirm the effectiveness of vesicle dissolution after heating (for the variable-temperature NMR experiments), CE experiments were performed on the supernatant from DCV samples prior to, and after, the heat-induced vesicle disintegration. Low-intensity electrophoretic peaks were detected in the supernatant from the sample prior to lysing (Figure 2A). After lysing the vesicles by heating the sample for 10 min at 90 °C, a significant increase in the amount of dissolved amino acids and peptides (Figure 2B) was detected, supporting the MS data and demonstrating the effectiveness of the lysis procedure.

Nuclear Magnetic Resonance Spectroscopy of Vesicle Suspensions. One-dimensional proton NMR experiments were performed on samples containing purified DCVs within 2 h of preparation. The vesicles were then lysed as described above. Visual observation by optical microscopy confirmed temperature-induced vesicle lyses. The downfield regions of the NMR spectra obtained before and after heating are shown in Figure 3A. The spectra exhibit several well-resolved peaks including the characteristic peaks of the internal standard, thimerosal (peaks 2 and 5). In the case of intact DCVs, the high-resolution NMR spectra showed no additional resonances besides the thimerosal and residual water peaks. Upon lysis, the appearance of new resonances suggests that some compounds become mobile after heating the vesicle suspension. Comparative analysis of standards and AG peptide structure information allows the assignment of

(19) Park, Y. H.; Zhang., X.; Rubakhin, S. S.; Sweedler, J. V. *Anal. Chem.* **1999**, *71*, 4997−5002.
(20) Zhang, X.; Fuller, R. R.; Dahlgren, R. L.; Potgieter, K.; Gillette, R.; Sweedler, J. V. *J. Anal. Chem.* **2001**, *369*, 206−211.
(21) Zhang, X.; Stuart, J. N.; Sweedler, J. V. *Anal. Bioanal. Chem.* **2002**, *373*, 332−343.

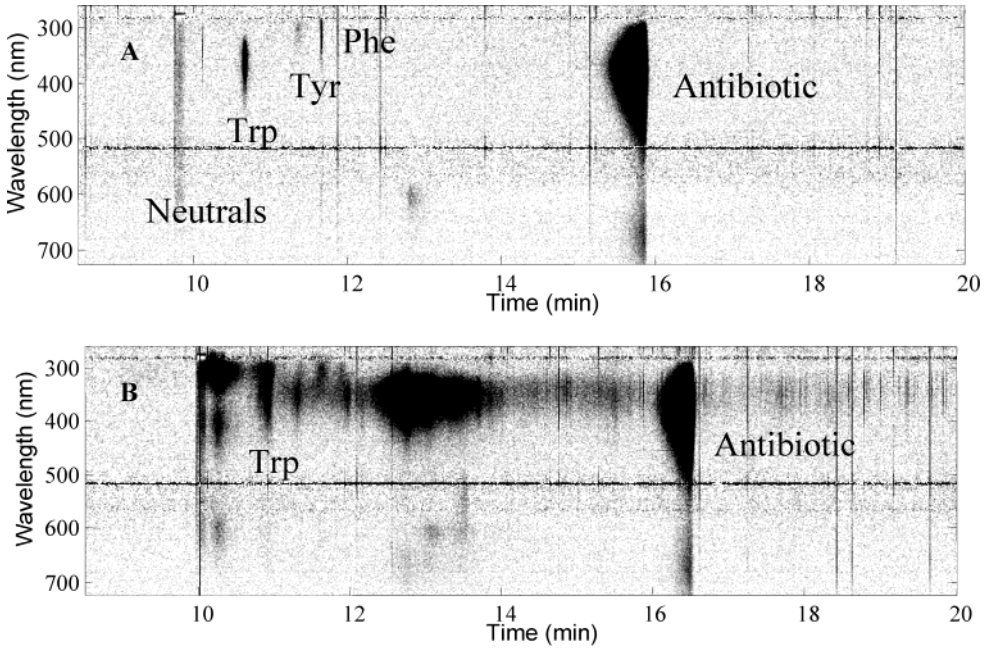

Figure 2. Gray scale wavelength-resolved fluorescence CE electropherograms of a vesicle suspension demonstrating the presence of a significant amount of Trp being released after heating. (A) Before heating. (B) After heating. Black areas represent eluting peaks that fluoresce, resolved along the ordinate by wavelength and along the abscissa by electrophoretic migration time. The run-to-run increase in electrophoretic migration time reflects the coating of the capillary walls with vesicular lipids and proteins slowing the electroosmotic flow. The large, unlabeled dark area in the bottom panel is from the detection of hundreds of unresolved proteins containing Trp and Tyr.

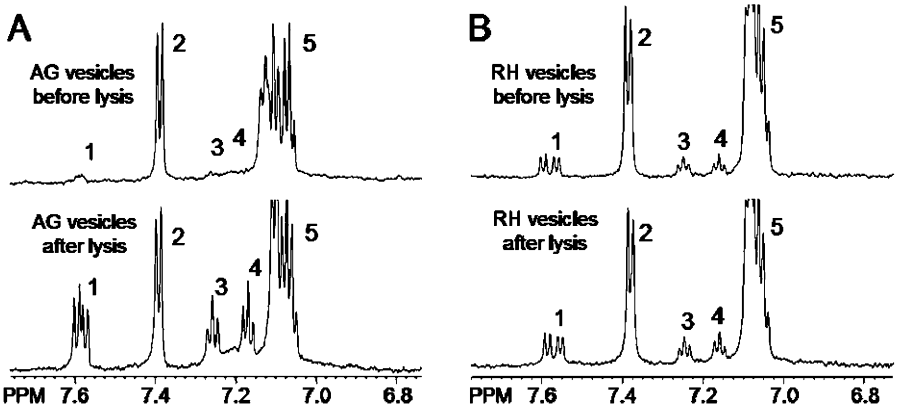

Figure 3. ^{1}H NMR spectra of DCVs and LVs in vesicular suspensions in phosphate buffer. (A) (top) intact AG vesicles; (bottom) lysed AG vesicles (after heating for 10 min at 90°C). (B) (top) intact RH vesicles; (bottom) lysed RH vesicles. A comparison of the two spectra from AG vesicles reveals the appearance of new NMR resonances upon heating. Little change is apparent for the corresponding spectra from the red hemiduct vesicles. Peaks 1, 3, and 4 have been assigned to the Trp aromatic ring. Peaks 2 and 4 are characteristic thimerosal resonances. Data acquisition parameters: spectral width 8000 Hz, number of complex data points 65 536, relaxation delay 2 s, and number of signal averages 200; 1-Hz line broadening was applied. NMR spectra shown are representative of six sets of experiments performed on DCVs and LVs.

peaks labeled 1, 3, and 4 to the tryptophan aromatic ring. Similar NMR experiments were performed on LVs suspended in phosphate buffer. Examples of spectra obtained before and after heating are shown in Figure 3B. In this case, the spectra are almost identical.

DISCUSSION

Results from MS and CE measurements of the AG vesicles confirm the presence of high concentrations of peptides within the DCVs and also indicate that the LVs appear nonpeptidergic. The NMR spectra from lysed DVCs contain typical solution-phase peaks, with several aromatic peaks assigned to Trp residues. What does the NMR analysis of intact DCVs tell us about the physical state of the Trp-containing molecules packaged inside the vesicles? NMR spectra of highly mobile species are characterized by narrow resonances, with the line widths limited by the spin−spin relaxation time.[22] Interactions such as chemical shift anisotropy, dipole−dipole interaction, and quadrupole interactions are averaged to zero due to the rapid isotropic molecular motion. Thus, typical line widths in pure liquids are less than 1 Hz. In solid materials, however, the anisotropic interactions do not average to zero and give rise to very broad NMR lines, typically several kilohertz. Without specific data acquisition strategies such as magic angle spinning [23,24] or multiple-pulse line narrowing,[25] NMR

(22) Abragam, A. *The principles of nuclear magnetism*; Clarendon Press: Oxford, U.K., 1961.
(23) Lowe, I. *Phys. Rev. Lett.* **1959**, *2*, 285−287.
(24) Andrew, E. R.; Bradbury, A.; Eades, R. G. *Nature* **1958**, *183*, 1802−1803.

spectroscopy of solidlike materials, including membrane-bound or precipitated peptides, does not give resolved resonances. The NMR results show that such a restricted environment is indeed present within the DCVs (the Trp peaks are nearly invisible prior to the vesicles being lysed) but not in the LVs.

As the NMR results are so important in reaching this conclusion, it is worth considering alternative mechanisms by which these resonances could be broadened. These include restricted diffusion of molecules within the vesicle and the diffusion of molecules across local magnetic field gradients, which are caused by the heterogeneity of the sample. In the case of restricted diffusion, one can think of a secretory vesicle as a sphere bounded by a membrane. If the spins inside the sphere diffuse in proximity to the membrane, then the internuclear dipolar interaction (which is not averaged to zero because of the restricted motion of the spins in the membrane) can reduce the effective transverse relaxation time (T_2^*) causing an increase in the line width (full width at half-maximum, $1/\pi T_2^*$). The time (t_{diff}) in which a molecule diffuses over a certain distance (λ) can be calculated from the Einstein equation: $\lambda^2 = 2Dt_{diff}$, where D is the effective diffusion coefficient. For water molecules (with $D = 2.5 \times 10^{-9}$ m^2/s), taking $\lambda \approx 1$ μm (the average distance that a molecule inside the vesicle diffuses until it interacts with membrane molecules) gives us $t_{diff} \approx 0.2$ ms, which will result in a line width of ~1.6 kHz. However, cellular metabolites and lipid molecules have diffusion coefficients in the range one-tenth to one-hundredth that of water, and therefore, the corresponding broadening is between 16 and 160 Hz. This simple calculation is supported by the fact that relatively narrow NMR resonances have been observed from artificial oil droplets [26] and cytosolic (1−2-μm diameter) lipid droplets in C6 cells[26,27] and that the immunogold studies demonstrated the packaging of the peptides in the dense core separated from vesicular membrane by lucent space.

The diffusion of molecules in the presence of magnetic field gradients due to sample heterogeneity can also lead to broad NMR lines.[28,29] However, for the particular geometry (spherically shaped vesicles) being studied, the magnetic field inside the vesicle is uniform even though the field profile outside the vesicles is disturbed.[30] Therefore, this mechanism is unlikely to result in significant line broadening.

CONCLUSIONS

A variety of analytical techniques have been used to investigate the physical state of the dense core of DCVs from *A. californica* and to compare the results to the case of LVs from the same organism. In the case of AG vesicles, we detect new NMR resonances after vesicle lysis by heating. In contrast, the RH vesicles do not show evidence of NMR-invisible contents in the intact form. These findings, along with the EM results, indicate that AG vesicles have a solid core packed with physiologically active peptides. These compounds may exist in a semicrystalline or a crystalline state in the dense vesicular interior. In contrast, in the case of the RH vesicles, the content appears to be relatively fluid and does not contain high amounts of peptides.

ACKNOWLEDGMENT

This work was supported by the National Institutes of Health (R01 EB02343 and R01 NS31609), the National Science Foundation (DBI-9722320), and the Alexander von Humboldt Stiftung.

Received for review November 13, 2003. Accepted February 4, 2004.

AC035346H

(25) Haeberlen, U.; Waugh, J. S. *Phys. Rev.* **1968**, *175*, 453−467.
(26) Perez, Y.; Lahrech, H.; Cabans, M. E.; Barnadas, R.; Sabes, M.; Remy, C.; Arus, C. *Cancer Res.* **2002**, *62*, 5672−5677.
(27) Hakumaki, J. M.; Kauppinen, R. A. *Trends Biochem. Sci.* **2000**, *25*, 357−362.
(28) Hansen, J. R.; Lawson, K. D. *Nature* **1970**, *225*, 542−544.
(29) Hansen, J. R. *Biochim. Biophys. Acta* **1971**, *230*, 482−486.
(30) Callaghan, P. T. *Principles of nuclear magnetic resonance microscopy*; Clarendon Press: Oxford, U.K., 1991.